

Shaking Table Tests of Steel Fiber Reinforced Concrete Walls for Housing



Julian Carrillo

Research professor, Universidad Militar Nueva Granada, UMNG, Bogota, Colombia.

Sergio M. Alcocer

Research professor, Universidad Nacional Autónoma de México, UNAM, Mexico, D.F.

José A. Pincheira

Associate professor, University of Wisconsin, Madison, USA.

SUMMARY:

Steel fiber reinforced concrete (SFRC) has exhibited suitable tension strength and post-cracking deformation capacities. Performance observed during tests prompts SFRC as a prominent raw material for construction of low-rise concrete wall housing in Latin America. In order to evaluate the contribution of steel fibers to shear strength and displacement capacities of concrete walls, as well as to assess the possibility of replacing the conventional web shear reinforcement of walls by steel fibers, shaking table tests of six concrete walls were carried out. Variables studied were the fiber aspect ratio (64 and 80) and fiber dosage expressed in terms of the minimum fiber dosage specified by ACI 318 (45, 60 and 75 kg/m³). The measured behavior of SFRC walls is also compared with that of conventionally reinforced walls.

Keywords: concrete walls, low-rise housing, steel fiber reinforced concrete.

1. INTRODUCTION

Low-rise reinforced concrete walls are a popular type of construction for family housing in Mexico and in other countries. Because of the large wall-to-floor area ratio, these walls use concrete strengths of 15 to 20 MPa and often require a minimum amount of both vertical and horizontal web shear reinforcement made of deformed bars or welded-wire mesh. Fabrication and installation of this minimum reinforcement in relatively thin walls (100 mm) is labor intensive and time consuming. When comparing the seismic demand and measured capacity of 39 walls used in typical one–two stories high concrete housing, Carrillo and Alcocer (2012) found that minimum web reinforcement prescribed by ACI 318 is overly conservative for controlling diagonal tension cracking, especially for structures located in low seismic hazard zones. For medium and low seismic hazard zones, it was suggested to reduce or disregard, respectively, the web shear reinforcement as long as suitable and specific methods for controlling shrinkage cracking, as well as allowable story drift ratios for limiting inclined cracking of concrete are used.

Previous studies (Kwak *et al.*, 2002; Parra-Montesinos, 2005; Ávila *et al.*, 2011) have shown that Steel Fiber Reinforced Concrete (SFRC) may increase both the shear strength and deformation capacities of structural elements. Based on performance observed in steel fiber reinforced concrete beams, ACI 318 (2011) allows using steel fibers for replacing the minimum area of conventional shear reinforcement in flexural members. To evaluate the contribution of steel fibers to both shear strength and the displacement capacities of low-rise concrete walls, as well as the possibility of replacing the conventional web shear reinforcement of walls by steel fibers, the behavior of six SFRC walls subjected to shaking table excitations is presented in this paper. Each wall was fabricated with a different type of SFRC that consisted of a different type of steel fiber and/or fiber volume. Aimed at studying the seismic performance under different limit states, from onset of cracking to collapse, specimens were subjected to three earthquake hazard levels. The initial period of vibration of the walls was established to agree with ambient vibration tests of typical low-rise housing. Wall performance is

presented in terms of the observed progression of cracks, hysteretic response and failure mode. The measured behavior of SFRC walls is also compared with that of conventionally reinforced walls.

2. REQUERIMENTS OF SFRC IN ACI 318

Fiber-reinforced concrete beams with hooked or crimped steel fibers in dosages of 60 kg/m³ have been shown to exhibit shear stresses larger than $0.17\sqrt{f'_c}$ MPa (Parra-Montesinos, 2006). In order to provide a design alternative to the use of shear reinforcement for members with longitudinal flexural reinforcement, ACI 318 (2011) allows using 60 kg/m³ of steel fibers for replacing the minimum area of conventional shear reinforcement in flexural members. ACI 318 allows this exception when normal-weight concrete is used, the specified compressive strength, f'_c , does not exceed 40 MPa, the height of the beam is not greater than 600 mm, and the factored shear stress is not greater than $\phi 0.17\sqrt{f'_c}$ MPa. In ACI 318, discontinuous deformed steel fibers are permitted for resisting shear in flexural members, unless the adequacy of the system is shown by tests. Steel discontinuous fiber reinforcement for concrete should be deformed and conform to ASTM A820 (2004). Additionally, steel fibers should have a length-to-diameter ratio not smaller than 50 and not greater than 100.

Today (2012), a third point load flexural test is the most representative and useful test method to assess the tensile properties of SFRC. Fig. 1 shows the typical flexural behavior of SFRC. In ACI 318, steel fiber reinforced concrete should be considered acceptable for shear resistance if the following conditions are also satisfied: (a) the residual strength obtained from flexural testing in accordance with ASTM C1609 (2005) at a mid-span deflection of $1/300$ of the span length, l_c , is greater than or equal to 90% of the measured first-peak strength obtained from a flexural test; and (b) the residual strength obtained from flexural testing in accordance with ASTM C1609 at a mid-span deflection of $1/150$ of l_c is greater than or equal to 75% of the measured first-peak strength obtained from a flexural test. SFRC should also conform to ASTM C1116 (2009).

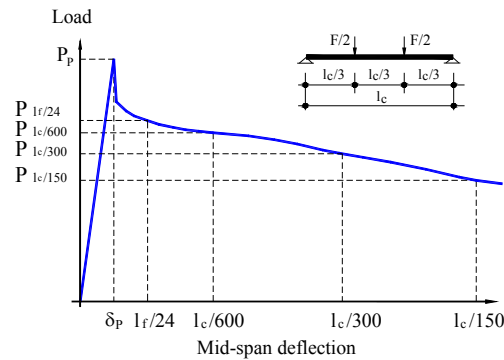


Figure 1. Typical load-deflection curve of SFRC using beam with third-point load.

Based on results of an experimental program of SFRC with fibers of different diameters, Dinh *et al.* (2010) have proposed different acceptance criteria. They recommended that the first deflection limit be based on fiber length, l_f , instead the span length, l_c , and different values of residual strengths. Therefore, Dinh *et al.* stated that SFRC should be considered acceptable for shear resistance if residual strengths obtained from flexural testing in accordance with ASTM C1609 (2005) at mid-span deflections of $1/24$ of l_f and $1/150$ of l_c are greater than or equal to 75% and 40%, respectively, of the measured first-peak strength obtained from a flexural test (Fig. 1).

3. EXPERIMENTAL PROGRAM

The three-dimensional prototype structure considered for this study was a two-story house built with reinforced concrete (RC) walls in the two principal directions. In this type of housing, 100-mm thick solid, cast in-place slabs are often used. Alternatively, slabs made of precast elements are also used.

Wall thickness and clear height are commonly 100 and 2400 mm, respectively, and house floor plan area varies between 35 and 65 m². Foundations are strip footings made of 400-mm square RC beams that support a 100-mm thick floor slab.

The experimental program included shaking table tests of six concrete walls with height-to-length ratio equal to one ($h_w/l_w = 1$). Variables studied were the fiber aspect ratio (length-to-diameter ratio, l_f/d_f) and fiber dosage expressed in terms of the minimum fiber dosage specified by ACI 318 ($D_{f-min} = 60 \text{ kg/m}^3$). Details of the steel fiber type and dosage used in the walls are shown in Table 1. Volume fraction was calculated as the ratio, in percentage, of fiber dosage in kg/m³ and steel density.

Table 1. Variables of the experimental program.

Variable	Description			
Steel fiber	Label	1F		2F
	Reference	Dramix RC-65/35-BN		Dramix RC-80/60-BN
	Type	Hook-ended		Hook-ended
	Length, l_f , mm	35		60
	Diameter, d_f , mm	0.55		0.75
	Aspect ratio, l_f / d_f	63.6		80.0
	Tensile strength, MPa (data sheet)	1100		1100
Dosage	% D_{f-min} :	75	100	125
	D_f (kg/m ³):	45	60	75
	Volume fraction, V_f %:	~ 0.55	~ 0.75	~ 1.00

Main characteristics of wall specimens are presented in Table 2. No conventional steel reinforcement or welded wire mesh was used in the web, i.e., only SFRC was used. Specimens were labeled to designate the type of fiber and the fiber volume as a fraction of that required by ACI 318 (2011). For instance, specimen MC1F100 was made using fiber type 1F and a dosage of 60 kg/m³ (100% of that required by ACI 318).

Table 2. Characteristics of specimens.

No.	Wall	Type of fiber	Dosage kg/m ³	% D_{f-min}	V_f %	t_w mm	l_w mm	h_w mm
1	MC1F75	1F	45	75	0.55	80	1920	1920
2	MC1F100	1F	60	100	0.75	81	1924	1921
3	MC1F125	1F	75	125	1.00	84	1925	1918
4	MC2F75	2F	45	75	0.55	82	1919	1925
5	MC2F100	2F	60	100	0.75	81	1917	1921
6	MC2F125	2F	75	125	1.00	81	1916	1920

3.1. Similitude requirements

Because of the limitations in the payload capacity of the shaking table at UNAM, lightly-reduced scaled models were designed and built (i.e. geometry scale factor, $S_L = 1.25$) for shaking table testing. The size of wall models was equal to 80% to that of walls in the prototype. The simple law of similitude was then chosen for scaling specimens. For this type of simulation, models are built with the same materials of the prototype and only the dimensions of the models are modified.

3.2. Geometry and reinforcement

Nominal geometry and reinforcement layout of the specimens are shown in Fig. 2. According to the scaling factors, height, length and constant thickness of walls were 1920, 1920 and 80 mm, respectively. Thus, height-to-length ratio was equal to one ($h_w/l_w = 1$). As-built wall dimensions are presented in Table 2. To prevent cracking during lifting, transportation and setting up of the specimens, wall models were built on a RC stiff grade beam. The foundation beam was anchored to the platform of the shaking table with prestressed rods. A top slab, cast monolithically with the walls, was used to connect the mass-carrying load system for testing (section 3.6).

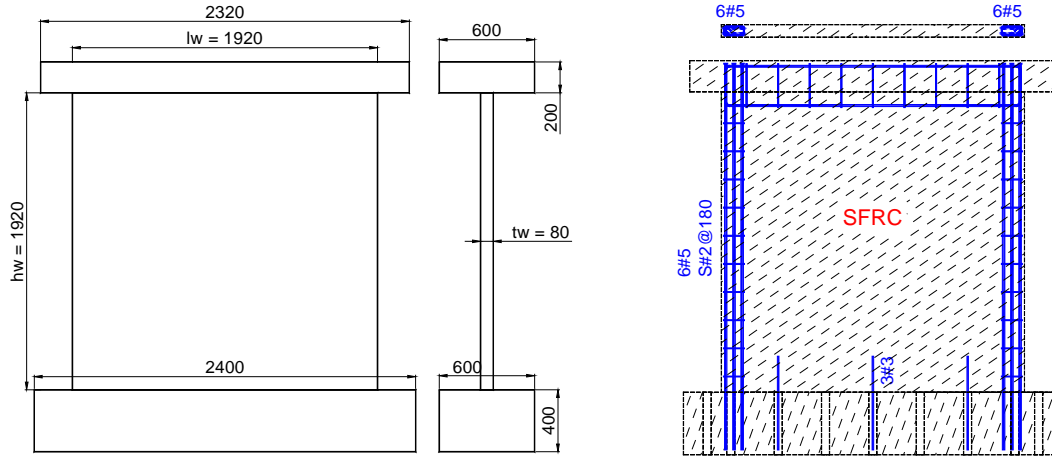


Figure 2. Geometry and reinforcement layout of specimens (dimensions in mm).

In the prototype house, all walls are connected to a RC solid slab, so that, top wall rotation is restrained. The behavior of these squat walls is primarily governed by shear deformations and hence the area of longitudinal reinforcement at boundary elements is almost always controlled by minimum flexural strength requirements. In the tests, top wall rotation was allowed (section 3.6), causing the wall to be bent in single curvature with the maximum bending moment at the base. To prevent flexural failure prior to achieving shear strength, the amount of the longitudinal reinforcement at the boundary elements was modified with respect to that encountered in walls of the prototype house. If the amount of longitudinal boundary reinforcement would have been similar to that used in prototype walls, a flexural failure would have been observed. Longitudinal and transverse reinforcement at the boundary elements consisted of 6 No. 5 deformed bars (15.9 mm diameter = 5/8 in.) with No. 2 smooth bar stirrups (6.4 mm diameter = 2/8 in.) spaced at 180-mm on center.

3.3. Mechanical properties of materials

The specified compressive strength of SFRC was 25 MPa, the same as that used in a typical RC wall. Maximum size of coarse aggregate was 10 mm. Casting of six walls was made using one type of concrete and two concrete mixes labeled as 1F for walls using 1F fibers and 2F for walls using 2F fibers (Table 2). SFRC was ready-mixed at the concrete plant with the lower dosage of fibers (45 kg/m³). For walls cast with 60 and 75 kg/m³ SFRC, a proper amount of steel fibers was added in-situ to the mix prior to pouring the SFRC into the forms. This was done to avoid using a different concrete mix with the same type of fiber. Mixing of steel fibers complied with manufactured recommendations, that is, a mixing rate was approximately 40 kg/min and mixing duration was the longer between 1 min/m³ and 5 minutes. This procedure was found to produce a mix with good workability with no clusters of fibers.

Mean value of the measured mechanical properties of the SFRC are presented in Table 3. Properties were obtained from compression and tensile splitting tests of standard cylinders and from 3-point bending tests of prismatic beams with 450-mm span length and 150-mm square section. All properties were measured on the same day the shaking table tests were conducted. Because of the small size of the coarse aggregate and the high measured slump, no internal mechanical vibration was needed. Form vibration was applied through a rubber hammer only. However, as was expected, workability of concrete decreased significantly as the fiber dosage augmented, particularly, when fibers with 60-mm long fibers were used. Residual strengths of SFRC specified by ACI 318 (2011) and Dinh *et al.* (2010) are also shown in Table 3.

Load-deflection relations obtained from flexural testing of SFRC with fiber type 1F and 2F are shown in Figs. 3 and 4, respectively. Four beam-type specimens were used for each fiber dosage. For comparison purposes, results of plain concrete (no fibers) of the same strength are included in these

graphs. The calculated toughness reported in Table 3 is a measure of the energy absorption capacity and is calculated as the area under the load-deflection curve up to a net deflection of 1/150 of the span (3.0 mm) using a specimen with a depth of 150 mm.

Table 3. Measured mechanical properties of SFRC.

Mechanical property		Concrete 1F				Concrete 2F			
		% D_{f-min}				% D_{f-min}			
		0	75	100	125	0	75	100	125
Slump, mm		*	210	180	170	*	210	200	180
Fiber dosage, D_f , kg/m ³		0	41.2	59.3	78.6	0	44.2	66.1	84.0
Compressive strength, f_c , MPa		*	22.2	21.0	20.3	35.6	31.1	30.8	30.7
Elastic modulus, E_c , MPa		*	9050	8508	8337	15857	10616	10615	12384
Tensile splitting strength, f_t , MPa		2.29	2.47	2.32	2.63	2.13	3.60	4.27	4.40
First-peak flexural strength, f_r , MPa		4.04	3.19	3.69	3.35	3.99	3.49	4.03	4.37
Maximum flexural strength, f_{max} , MPa		4.04	3.23	3.69	3.96	3.99	3.49	4.42	5.41
f_{lf24}/f_r		0	0.72	0.81	1.12	0	0.69	0.96	1.07
f_{lc300}/f_r		0	0.72	0.80	1.12	0	0.79	1.02	1.17
f_{lc150}/f_r		0	0.65	0.65	0.85	0	0.66	0.94	1.02
Toughness, T , Joule		16.5	52.2	64.0	76.1	12.3	59.2	87.1	109.6
Compliance of residual strengths	ACI 318	---	No	No	Yes	---	No	Yes	Yes
	Dinh <i>et al.</i>	---	No	Yes	Yes	---	No	Yes	Yes

* Data not available.

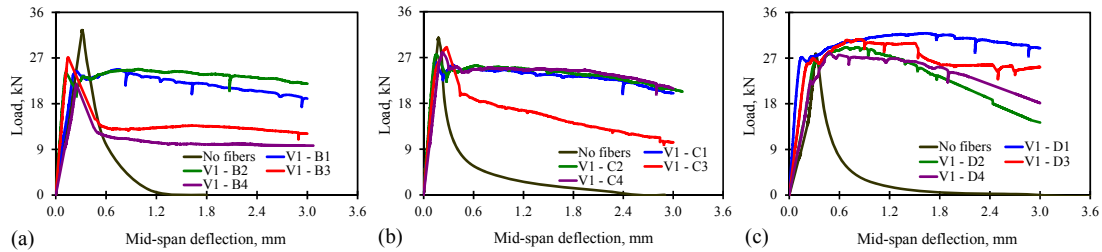


Figure 3. Load-deflection curves of SFRC with fibers 1F.

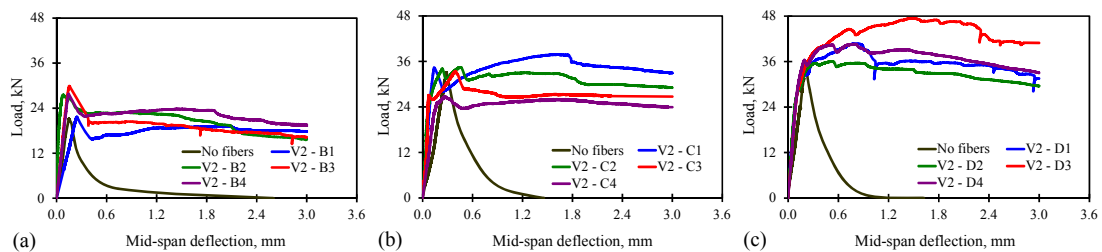


Figure 4. Load-deflection curves of SFRC with fibers 2F.

3.4. Loading histories

To assess wall performance under ground motion, the walls were subjected to real and artificially generated acceleration records. To compare the behavior of the low-rise SFRC walls with that of conventionally reinforced walls, the same earthquake records used in a previous experimental program were used (Carrillo and Alcocer, 2012). Records of different hazard levels were chosen so as to induce increasing levels of damage to the walls (from onset of cracking to collapse). The earthquake recorded in *Caleta de Campos* station, Mexico, in January 11, 1997 ($M_W=7.1$, CA-71) has a PGA of 0.38 g and was expected to cause diagonal cracking but no major damage to the walls. Such a record was measured in the epicentral region nearby Acapulco. The CA-71 record was considered as a Green

function to simulate larger-magnitude events. Two earthquakes with magnitudes M_w 7.7 (CA-77) and 8.3 (CA-83) were numerically simulated for the strength and ultimate limit states, respectively.

According to the simple law of similitude, acceleration and time scale factors were applied to the records for testing of models. Specimens were tested under progressively more severe earthquake demands, by increasing the peak acceleration of the record until substantial loss of lateral strength or excessive lateral displacements occurred. Walls were tested in the in-plane direction only. Target PGA and the sequence of input motion used in the tests are described in Table 4. At the beginning and at the end of the tests, a random acceleration signal (white noise, WN) at 10 cm/s^2 (0.01 g) root mean square (RMS) was also applied to identify the periods of vibration and the damping factors of models.

Table 4. Testing stages for the prototype house.

Stage	Record	Peak ground acceleration, PGA		Total duration, s
		%	g	
1	WN	---	0.01	120.0
2	CA-71	50	0.19	29.5
3		100	0.38	
4	CA-77	75	0.54	36.1
5		100	0.72	
6	CA-83	75	0.98	99.8
7		100	1.30	
8		150	1.95	
9		200	2.60	
10	WN	---	0.01	120.0

3.5. Design for dynamic similitude

The fundamental period of vibration of the two-story prototype house was estimated to be 0.12 s (Carrillo and Alcocer, 2012). Taking into account the scale factors of the simple law of similitude, isolated wall models were designed to achieve an initial in-plane period of vibration of approximately 0.10 s ($0.12 \text{ s} / 1.25$). The dynamic weight (mass \times gravity acceleration) needed to achieve the desired design period was calculated to account for the reduced stiffness due to early-age cracking. The dynamic weight used for achieving the desired design periods of walls with steel fibers 1F and 2F was 175.6 kN and 231.4 kN, respectively.

3.6. Test setup and instrumentation

Fig. 5 shows the test setup and instrumentation used in the tests. In this setup, the mass-carrying load system proposed by Carrillo and Alcocer (2011) for supporting the mass and transmitting the inertia forces was used. The device allows guided horizontal sliding of the mass within a fixed supporting structure installed outside the shaking table. This was done to avoid the risk of lateral instability due to the mass self-weight required for adequate dynamic simulation. Mass blocks (dynamic weight) were placed in a steel box which is, in turn, supported by a linear motion guide system (LMGS) with very low friction (Fig. 5a).

An axial compressive stress of 0.25 MPa was uniformly applied to the walls and kept constant during testing. This value was selected to correspond to the typical axial stress level found in the first story of the prototype house (Carrillo and Alcocer, 2012). During the tests, the axial load was exerted through the weight of the load and connection beams, plus lead ingots bolted to the load beam. Although lead ingots resulted in a triangular load distribution, the addition of the weight of the connection beam provided for a uniform distribution of the axial load on the walls (Fig. 5a).

To measure the specimens' response, walls were instrumented internally and externally (Fig. 5). Internal instrumentation was designed to acquire data on the local response of longitudinal deformed bars in the boundary elements through strain-gages at selected locations (Fig. 5b). External

instrumentation was planned for measuring both the tensile strain demand at SFRC through strain-gages mounted on the wall web surface and the global response through displacement, acceleration and load transducers. The load exerted on the specimens by the moving mass of the external device was measured by a load cell attached to the connection beam at the top of the walls (Fig. 5a). Also, an optical displacement measurement system with Light Emitting Diodes (LED) mounted on the wall surface was used to measure the displacement field at 0.01 s intervals. In the tests, 41 strain-gages for steel reinforcement, 8 strain-gauges for SFRC and 43 external transducers were used.

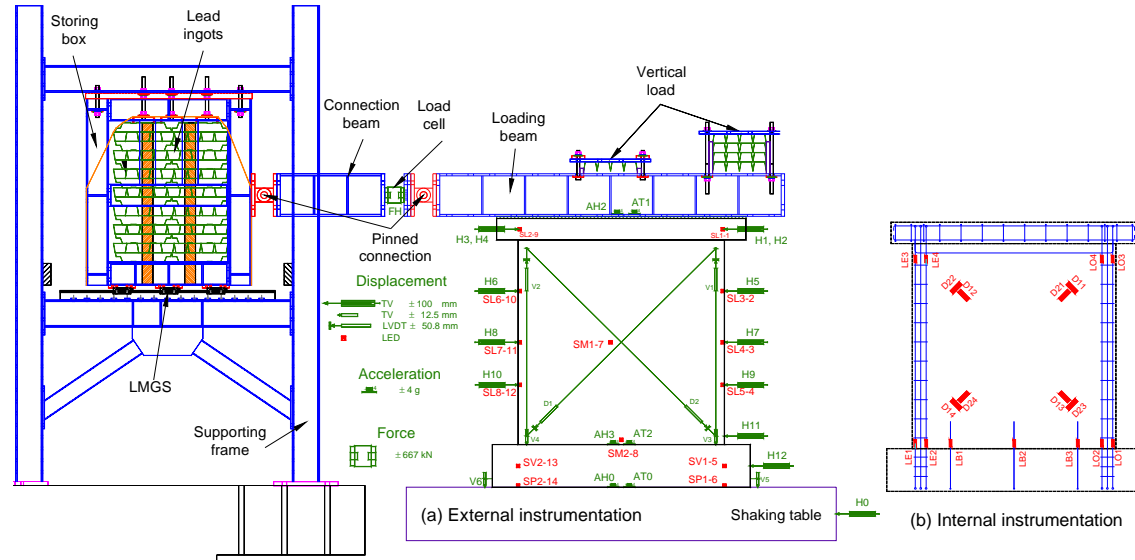


Figure 5. Test setup and instrumentation.

4. TEST RESULTS AND DISCUSSION

4.1. Crack patterns

Prior to testing, walls exhibited early-age cracking. Crack width was smaller than 0.05 mm. Based on the location and slope of the cracks, they are believed to be due to early-age shrinkage restrained by the longitudinal reinforcement at the boundary elements. Typical crack patterns at the peak shear strength of all walls are shown in Fig.6. The maximum lateral drift ratio, R , attained at peak shear strength is also shown in the figure. The drift ratio, R , was calculated by dividing the relative displacement measured at mid-thickness of the top slab by the height at which such displacement was measured. The drift ratio corresponded to the average of the peak values measured in each direction of displacement.

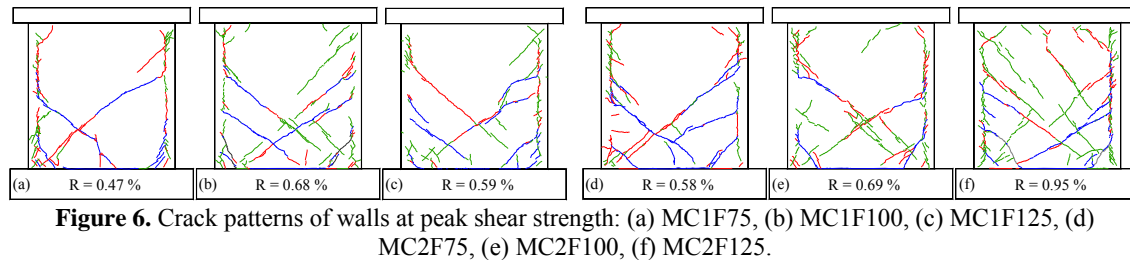


Figure 6. Crack patterns of walls at peak shear strength: (a) MC1F75, (b) MC1F100, (c) MC1F125, (d) MC2F75, (e) MC2F100, (f) MC2F125.

Fig. 6 shows that some flexural cracks were observed at boundary elements. Although a sliding crack at the join of wall web and foundation beam was detected in all walls, residual width of this crack remains almost constant during all testing stages. Web inclined cracks were observed in all walls, particularly at the lower half of wall web. The average value of crack inclination vary between 37° and

42° for walls with fiber type 1F, but it was roughly constant and equal to 40° for walls with fiber type 2F. Diagonal cracking was concentrated mainly at two or three major inclined cracks in all walls but specimen MC2F125 (see Fig. 6f). As was expected, more diagonal cracks of smaller width were observed as the fiber dosage was increased, irrespective of the fiber type. This trend has been also observed during testing of both walls rehabilitated using an additional thickness of SFRC (Ávila *et al.*, 2011) and SFRC beams (Schumacher *et al.*, 2009).

To compare the effect of the fiber type, it is apparent in Fig. 6 a better uniform distribution of web cracking in walls with fiber 2F ($l_f/d_f=80$) when compared with that observed in walls with fiber 1F ($l_f/d_f=64$). This fact is associated to the better shear performance of steel fibers with higher aspect ratios (Figs. 3 and 4). In general, fewer diagonal cracks of greater width were observed when compared with similar low-rise concrete walls with conventional web reinforcement (Carrillo and Alcocer, 2012), that is, better distribution of cracks is achieved when web shear reinforcement is made of welded-wire mesh or deformed bars. It is also observed in Fig. 6 that a significant area of the facade of walls remained intact during all testing stages. This trend was more evident for walls with lower dosages of steel fibers.

4.2. Observed failure mode

All walls exhibited a diagonal tension failure mode. Failure was sudden and was triggered by the abrupt and excessive opening of one or two of the major diagonal cracks in the web. At the end of tests, walls were essentially divided into two or four segments. Forensic examination of the walls revealed that opening of the main diagonal cracks was caused by pull-out of steel fibers across the width and length of the crack. No fracture of the steel fibers was observed. Therefore, the behaviour of steel fiber was controlled by stretching of hooks at the ends of the fibers.

After attaining shear failure, major web inclined cracks penetrated into the wall boundary elements causing crushing and spalling of concrete as well as yielding of longitudinal reinforcement near the wall base. Subsequently, an effect similar to that of captive columns was observed at the upper part of boundary elements. In general, boundary elements provided confinement to the wall web and avoided the total loss of gravity-load carrying capacity at ultimate. Crack patterns of walls with fiber type 2F at ultimate are shown in Fig. 7. Similar crack patterns were observed in walls with fiber type 1F. Although, in theory, it is likely to attain diagonal compression failures in low-rise SFRC walls, two issues prevent reaching of shear failures governed by crushing of concrete: focussing of damage in some major web inclined cracks and the limited capacity of displacement when compared with concrete walls reinforced with the minimum amount of web shear reinforcement specified by ACI 318 and using deformed bars (Carrillo and Alcocer, 2012).



Figure 7. Final crack patterns of walls with fiber type 2F: (a) MC2F75, (b) MC2F100, (c) MC2F125.

4.3. Hysteretic response

The behavior of the walls was also assessed from the measured hysteretic response expressed in terms of a normalized shear stress, and lateral drift ratio, R . The measured lateral load was divided by the

wall gross area to compute an average shear stress. As-built wall thickness and wall length were used to calculate the wall gross area (Table 2). Because diagonal tension was the dominant failure mode, a normalized shear stress computed as the average shear stress divided by the tensile splitting strength of the plain concrete (f_t , see Table 3) is also provided in the plots. Effective lateral force was obtained using the equations proposed by Carrillo and Alcocer (2011), which are applicable when the mass-carrying load system is that shown in Fig. 5a. The hysteresis curves of all walls are shown in Fig. 8.

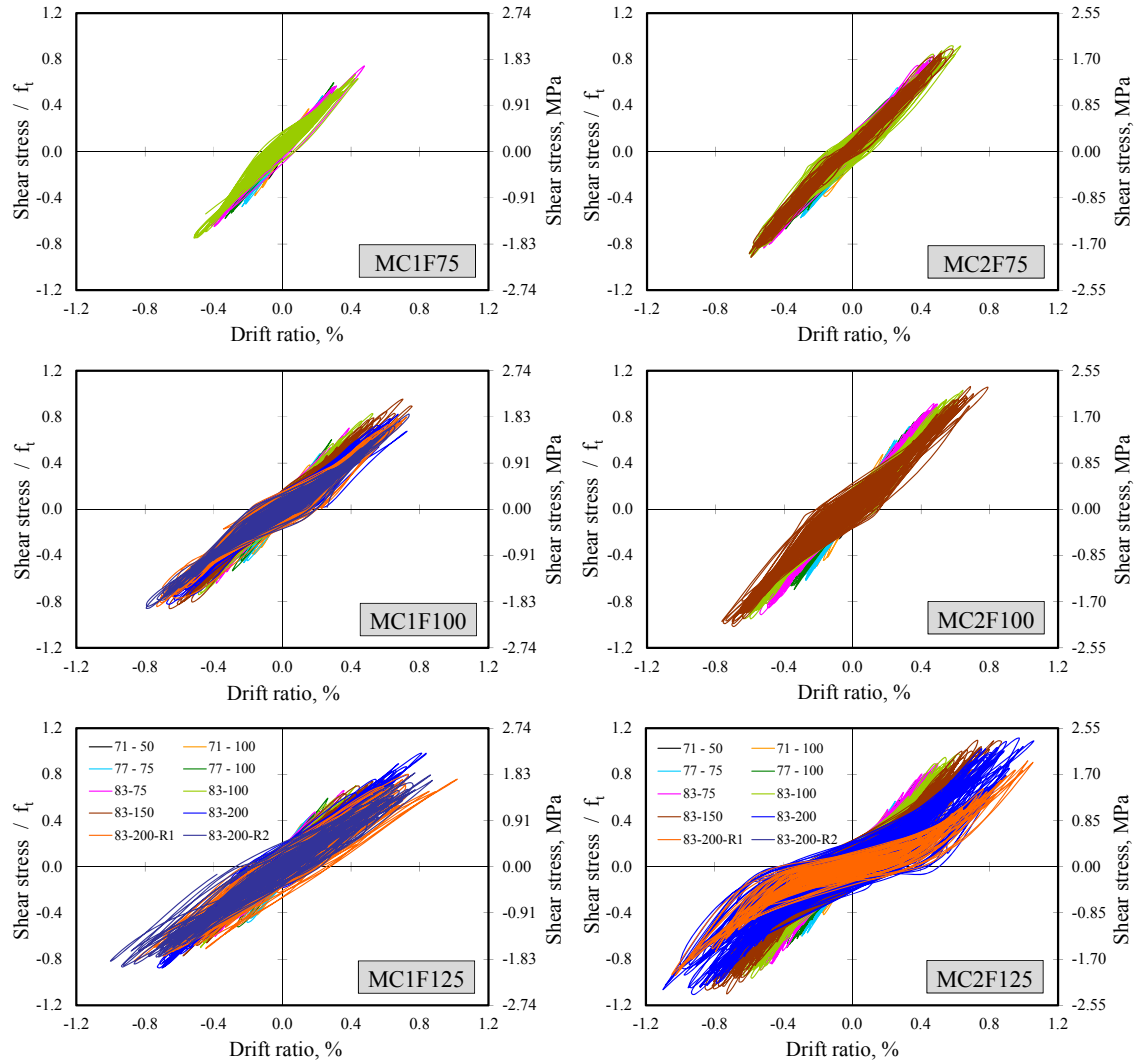


Figure 8. Hysteresis curves.

As shown in Fig. 8, the hysteresis loops were highly pinched as is typical of low-rise concrete walls dominated by shear deformations. Hysteresis loops were stable and nearly symmetric during all testing stages until the abrupt failure of the walls. Moreover, pinching of hysteresis loops was evident but lower than that observed in low-rise concrete walls reinforced for web shear using conventional reinforcement. Therefore, the confinement effect that steel fibers provided to concrete and the low level web cracking could have a favorable effect in the energy dissipation capacity of low-rise steel fiber reinforced concrete walls. However, the inelastic portion of the curves was limited, particularly for walls with fiber dosages lower than the minimum dosage specified by ACI 318 (60 kg/m^3). For these walls, ultimate displacement capacity was nearly equal to that at peak shear strength, showing values of drift demands lower than 0.8%. In general, the hysteretic behavior of those walls ($D_f < 60 \text{ kg/m}^3$) was similar to that observed in concrete walls reinforced for web shear using welded-wire meshes (Carrillo and Alcocer, 2012). For walls with $D_f \geq 75 \text{ kg/m}^3$, values of drift demands close

to 1.0% were recorded. In all walls, the ultimate limit state was defined as that corresponding to a drop of the peak shear strength of 20% or lower.

5. FINAL REMARKS

In this study, the seismic performance of Steel Fiber Reinforced Concrete (SFRC) walls as an alternative to conventionally reinforced low rise walls was presented. When comparing crack patterns of SFRC walls, they were observed more diagonal cracks of smaller width as the fiber dosage was increased, and better uniform distribution of web cracking as the aspect ratio of the fiber was higher. However, better distribution of cracks is achieved when web shear reinforcement is made of welded-wire mesh or deformed bars. In addition, the lower pinching of hysteresis curves of SFRC walls suggest that the confinement provided by steel fibers to concrete and the low level web cracking, helped to improve the energy dissipation capacity of the walls. Moreover, strength and displacement capacities were similar to that observed in concrete walls reinforced for web shear using welded-wire mesh. Therefore, the results of this study show that SFRC walls can exhibit a performance comparable to that of conventionally reinforced walls in terms of strength and deformation capacities under seismic induced loading. Additional work is underway to develop a backbone model for predicting the load-displacement response and, to develop design provisions for minimum steel fiber dosage as an alternative to the minimum web shear reinforcement of concrete walls for low-rise housing.

ACKNOWLEDGEMENT

The authors gratefully acknowledge the support of construction materials from Cemex Group (concrete) and Bekaert (steel fibers), as well as the extensive assistance in the experimental testing of staff and students of the Structural Engineering Laboratories of the Instituto de Ingeniería at UNAM. The first author expresses his gratitude to the Universidad Militar Nueva Granada (UMNG, Colombia) for granting academic and research scholarships.

REFERENCES

- ACI Committee 318 (2011). Building code requirements for structural concrete (ACI 318-11) and commentary (ACI 318R-11). *American Concrete Institute*, Farmington Hills, Mich., 465.
- ASTM-A820 (2004). Standard specification for steel fibers for fiber-reinforced concrete. West Conshohocken, PA, USA, 4 pp.
- ASTM-C1116 (2009). Standard specification for fiber-reinforced concrete. West Conshohocken, PA, USA, 7 pp.
- ASTM-C1609 (2005). Standard test method for flexural performance of fiber-reinforced concrete (using beam with third-point loading). West Conshohocken, PA, USA, 8 pp.
- Ávila, O., Carrillo, J. and Alcocer, S. (2011). Rehabilitation of concrete walls using steel fiber reinforced concrete (SFRC): Shaking table tests, *Investigación y Desarrollo* **2:2**, 2-17 (in Spanish)
- Carrillo, J. and Alcocer, S. (2012). Seismic performance of concrete walls for housing subjected to shaking table excitations. *Engineering structures* **41**, 98-107.
- Carrillo, J. and Alcocer, S. (2011). Improved external device for a mass-carrying sliding system for shaking table testing. *Earthquake Engineering and Structural Dynamics* **40:4**, 393-411.
- Dinh, H., Parra-Montesinos, G. and Wight, J. (2010). Shear behavior of steel fiber-reinforced concrete beams without stirrup reinforcement. *ACI Structural Journal* **107:5**, 597-606.
- Kwak, Y., Eberhard, M., Kim, W. and Kim, J. (2002). Shear strength of steel fiber reinforced concrete beams without stirrups. *ACI Structural Journal* **99:4**, 530-538.
- Parra-Montesinos, G. (2006). Shear strength of beams with deformed steel fibers. *Concrete International* **28:11**, 57-66.
- Parra-Montesinos, G. (2005). High-performance fiber reinforced cement composites: an alternative for seismic design of structures. *ACI Structural Journal* **102:5**, 668-675.
- Schumacher, P., Walraven, J., Uijl, J. and Bigaj-van, A. (2009). Rotation capacity of self-compacting steel fibre reinforced concrete beams. *HERON Journal* **54:2**, 101-125.